Articles in PresS. Am J Physiol Lung Cell Mol Physiol (March 25, 2016). doi:10.1152/ajplung.00367.2015

ABSENCE OF TNF-α ENHANCES INFLAMMATORY RESPONSE IN THE NEWBORN LUNG UNDERGOING MECHANICAL VENTILATION

Harald Ehrhardt[1*], Tina Pritzke[2*], Prajakta Oak[2], Melina Kossert[2], Luisa Biebach[3], Kai Förster[3], Markus Koschlig[2], Cristina M. Alvira[4], Anne Hilgendorff [2, 3]

[1]Department of General Pediatrics and Neonatology, University Hospital of Giessen and Marburg, Giessen (UGMLC), Germany, Member of the German Lung Research Center (DZL)

[2]Comprehensive Pneumology Center, Helmholtz Zentrum Muenchen, Munich, Germany, Member of the German Lung Research Center (DZL)

[3]Department of Neonatology, Dr. von Haunersches Children`s Hospital, Ludwig-Maximilians University of Munich, Munich, Germany

[4]Dept. of Pediatrics, Stanford University, Stanford, California, USA

[*] The authors equally contributed to the study and preparation of the final manuscript.

Running title: Increased inflammation in ventilated newborn TNF-α null mice

Address correspondence to: Anne Hilgendorff, MD
Comprehensive Pneumology Center
Helmholtz Zentrum Muenchen
Max-Lebsche Platz 31
81377 Munich
Telephone: +49-89-3187-4675
Fax: +49-89-3187-4661
E-mail: anne.hilgendorff@med.uni-muenchen.de

ABSTRACT

Rationale: Bronchopulmonary dysplasia (BPD), characterized by impaired alveolarization and vascularization in association with lung inflammation and apoptosis, often occurs after mechanical ventilation with oxygen rich gas (MV-O_2). As heightened expression of the pro-inflammatory cytokine TNF-α has been described in infants with BPD, we hypothesized that absence of TNF-α would reduce pulmonary inflammation, and attenuate structural changes in newborn mice undergoing MV-O_2.

Methods: Neonatal TNF-α null (TNF-$\alpha^{-/-}$) and wild type (TNF-$\alpha^{+/+}$) mice received MV-O_2 for 8h; controls spontaneously breathed 40%O_2. Histologic, mRNA and protein analysis in vivo were complemented by in vitro studies subjecting primary pulmonary myofibroblasts to mechanical stretch. Finally, TNF-α level in tracheal aspirates (TA) from preterm infants were determined by ELISA.

Results: Although MV-O_2 induced larger and fewer alveoli in both, TNF-$\alpha^{-/-}$ and TNF-$\alpha^{+/+}$ mice, it caused enhanced lung apoptosis (TUNEL, Caspase-3/-6/-8), infiltration of macrophages and neutrophils, and pro-inflammatory mediator expression (IL-1β, CXCL-1, MCP-1) in TNF-$\alpha^{-/-}$ mice. These differences were associated with increased pulmonary TGF-β signaling, decreased TGF-β inhibitor SMAD-7 expression and reduced pulmonary NF-κB activity in ventilated TNF-$\alpha^{-/-}$ mice. Preterm infants who went on to develop BPD showed significantly lower TNF-α levels at birth.

Conclusion: Our results suggest a critical balance between TNF-α and TGF-β signaling in the developing lung, and underscore the critical importance of these key pathways in the pathogenesis of BPD. Future treatment strategies need to weigh the potential benefits of inhibiting pathologic cytokine expression against the potential of altering key developmental pathways.

Keywords: Tumor necrosis factor, TNF-α, neonatal chronic lung disease, bronchopulmonary dysplasia, mechanical ventilation, newborn mice, lung, TGF-β, apoptosis

INTRODUCTION

Chronic lung disease in the preterm infant, Bronchopulmonary Dysplasia (BPD), is the most frequent chronic lung disease in infancy. The development of BPD is associated with severe respiratory infections, reactive airway disease and limitations of pulmonary function that persist into adulthood (7). BPD is characterized by disrupted alveolarization and abnormal development of alveolar capillaries with variable degrees of interstitial cellularity, elastic fiber deposition and fibroproliferation (19). The characteristic pulmonary inflammatory response induced by mechanical ventilation (MV) and oxygen toxicity is a central contributor to the pathologic changes observed in BPD, as evidenced by an induction of pro-inflammatory cytokines and an increased influx of macrophages and neutrophils (2, 17, 33). Clinical and experimental studies have shown that the up-regulation of pro-inflammatory cytokines such as interleukin (IL) -1β, IL-6, IL-8 and TNF-α, correlates with the development of BPD (6, 35), and conversely that patients with BPD demonstrate decreased expression of anti-inflammatory cytokines (e.g. IL-10), and growth factors critical for vascular and alveolar development (e.g. vascular endothelial growth factor-A (VEGF-A) and platelet derived growth factor-A (PDGF-A) (30).

Increased expression of TNF-α plays a key role in severe infections and many inflammatory diseases in children and adults, and therapeutic strategies targeting excess TNF-α have been proven effective for many of these conditions (22, 27). TNF-α signaling activates the pro-inflammatory nuclear factor kappa-B (NFκB) pathway, resulting in the augmentation and perpetuation of the inflammatory response, and an increase in apoptosis (21).

Elevated levels of TNF-α have been found in preterm infants who later developed BPD (2, 17, 30, 35), however, the specific function of this cytokine in the pathogenesis of BPD

78 remains unclear. In order to investigate TNF-α in the pathophysiologic context of BPD and
79 determine its potential as a therapeutic target, we studied TNF-α expression levels in BPD
80 patients, and evaluated its pathophysiologic consequences in a mouse model of BPD. MV
81 with oxygen-rich gas (MV-O_2) triggers the onset and progression of BPD in association with a
82 characteristic inflammatory response, therefore we studied whether the absence of TNF-α in
83 the newborn mouse lung undergoing MV-O_2 decreases inflammation and apoptosis, thereby
84 improving lung structure. *In vitro,* we performed experiments to study the restoration of TNF-α
85 signaling in mouse primary lung MFBs. In order to translate these findings observed in our
86 experimental models to the clinical setting, we measured TNF-α expression in tracheal
87 aspirates of preterm infants prior to, and during MV-O_2, in order to determine whether MV-O_2
88 in the preterm infant leads to significant changes in TNF-α levels associated with the
89 development of BPD.

METHODS

For a more detailed description of the methods applied please refer to the online supplement.

Newborn mouse ventilation

Transgenic Mice. Transgenic mice and WT controls were purchased from Jackson laboratories (Bar Harbor, Maine, USA) provided by Charles River (Sulzfeld, Germany). TNF- α deficient mice have not been described with an abnormal pulmonary phenotype.

Mechanical Ventilation Experiments. 6-7-day-old C57B/6J wild type (WT, TNF-$\alpha^{+/+}$) and TNF-α knock-out (TNF-$\alpha^{-/-}$) mice born at term gestation (WT 3.8 ± 0.52 g; TNF-$\alpha^{-/-}$ 4.0 ± 0.37 g bodyweight (bw) were randomly selected to either receive MV-O_2 for 8h (fiO_2 0.4) or to spontaneously breathe 40% O_2 for 8h (4-8 mice per group). Mice selected for ventilation underwent a tracheotomy after sedation with ketamine (~60 µg/g body weight, bw) and xylazine (~12 µg/g bw), followed by MV-O_2 at 180 breaths/min from a customized, small animal respirator (MicroVent 848; Harvard Apparatus, Holliston, MA) for 8h. The ventilation protocol was designed to minimize baro- and volutrauma and thereby mimic clinical settings (mean tidal volume 8.68 µl/g bw; airway pressures: peak 12-13 cmH_2O, mean 11-12 cmH_2O). Newborn WT and TNF-$\alpha^{-/-}$ control mice, spontaneously breathing 40% oxygen received sham surgery under mild sedation. The ventilation procedure has been published previously (15). At the end of each study, pups were euthanized with sodium pentobarbital and lungs were harvested for further analysis. All animals were viable with response to tactile stimulation and adequate perfusion at the end of each experiment. All surgical and animal care procedures and experimental protocols were reviewed and approved by the local Institutional Animal Care and Use Committee of the Regierung von Oberbayern.

Tissue Assays

Processing lungs for quantitative histology. Lungs (n=6-8/group) were fixed intra-tracheally with buffered 4% paraformaldehyde overnight at 20 cmH_2O, as previously

described (3). Volume of fixed lungs was measured by fluid displacement (28). After paraffin embedding and isotropic uniform random (IUR) sectioning (28), quantitative assessment of alveolar area and number of incomplete and complete alveolar walls (septal density) was performed in 2-3 independent random tissue sections (4 µm, H&E) per animal (CAST-Grid 2.1.5; Olympus, Ballerup, Denmark). Radial alveolar counts were assessed ≥ 30 fields of view in 2-3 independent random tissue sections per animal (13).

Assessment of PDGF-Rα positive cells and related apoptosis in distal lung. PFA-fixed lung tissue sections were stained for PDGF-Rα (C-20) (Santa Cruz Biotechnology #sc-338), cleaved Caspase-3 (Cell Signaling Technology #9661S), and DAPI (Sigma Aldrich #D8417) in combination. Double-positive cells were quantified in 8 different fields of view/animal (400x magnification) using the Imaris Software (Imaris Software, Zurich, Switzerland).

Protein extraction and immunoblot analysis. Lungs from 8h studies (n=4/group) were excised, weighed and stored at -80°C for later protein extraction using high urea buffer (KPO_4, Urea, AppliChem, Darmstadt, Germany) and Halt Protease Inhibitor Cocktail (catalog #1861280, Thermo Fisher Scientific). After measurement of protein concentrations (BCA, catalog #23227, Pierce Scientific Rockford, IL, USA) immunoblots were performed using a Bis-Tris (catalog #NP0321BOX, Life Technologies, Darmstadt, Germany) or a Tris-Acetate (catalog #EA0375BOX, Life Technologies) gel as published previously (15) using the following antibodies: Caspase-3 (catalog #9662S, Cell Signaling), cleaved Caspase-3 (catalog #9661, Cell Signaling Technology), cleaved Caspase-6 (catalog #9761S, Cell Signaling), Caspas-8 (catalog #3259-100 Bio Vision), pSMAD 2 (catalog #3101S, Cell Signaling), SMAD 2/3 (catalog #3102S, Cell Signaling), SMAD 7 (catalog #sc-9183, Santa Cruz Biotechnology) β-actin (catalog #sc-81178, Santa Cruz Biotechnology); secondary antibody goat anti-mouse

IgG (catalog #2060, Santa Cruz Biotechnology) secondary antibody goat anti-rabbit IgG (catalog #2301, Santa Cruz Biotechnology) or donkey anti-goat IgG-HRP (catalog #2020, Santa Cruz Biotechnology) conjugated to horseradish peroxidase. Images were detected by chemiluminescence (catalog #RPN2232, GE Healthcare, Buckinghamshire, Great Britain) and quantified by densitometry (Bio Rad, Munich, Germany).

RNA extraction and quantitative real-time PCR. After mRNA extraction (catalog #A979.1, Carl Roth GmbH) and purification (catalog #12-6834-01, Peqlab, Erlangen, Germany) quantitative real-time PCR was applied to measure lung mRNA expression of IL-1β, CXCL-1 and MCP-1 using proprietary primer-probes (Eurofins mwg operon, Ebersberg, Germany).

In vitro studies

Mouse primary (myo)fibroblasts. Mouse MFBs were extracted from PBS-flushed lungs of 5-7 day old C57B/6J WT mice and cultured on a petridish (Corning #430167, Tewksbury MA, USA) in media (catalog #41966-029, Gibco, Darmstadt, Germany) containing Pen/Strep (catalog #15140-122, Gibco) and Gentamycin (catalog #BE02-012E, Lonza, Basel, Switzerland). FACS analysis of primary mouse lung MFBs showed the following characterization: 77.2±14% PDGF-Rα$^+$Vimentin$^+$, 16.7±12% Vimentin$^+$, 77.6±27% αSMA$^+$, 32±8.6% CD90$^+$, 8.5± 4.5% CD105$^+$. In addition, the analysis showed a negligible amount of leucocytes (0.6±0.5% CD45$^+$).

Mechanical stretch experiments. Primary mouse lung MFBs were seeded on flexible-bottomed laminin-coated culture plates (Flex Cell International Corporation catalog no.: BF-3001L) to undergo *in vitro* stretch in room air at 70-80% confluence (cyclic strain by vacuum pressure: shape / sine; elongation min 2%, max 8%; frequency 2Hz; duty cycle 50%; cycles 43216; duration 24h) for 24h. Treatment with TNF-α was performed using 100 ng/ml

recombinant TNF-α (Pepro Tech catalog #300-01A). The stretch experiment was started right after adding TNF-α treatment. At the end of each experiment, cells were harvested in 60 µl of RIPA buffer (150 mM NaCl, (catalog #A2942 AppliChem), 10 mM Tris-buffer pH 7.2, (catalog #A1379 AppliChem), 0.1% SDS, (catalog #A1502, AppliChem), 1% Triton X 100, (catalog #3051.2, Carl Roth), 1% Sodium Deoxycholate, (catalog #D6750 Sigma), 5 mM EDTA, (catalog #A3562 AppliChem)) including Halt Protease Inhibitor Cocktail (catalog #1861280, Thermo Fisher Scientific).

TNF-α cytokine levels in tracheal aspirate samples of preterm infants.

Tracheal aspirates were obtained at birth from preterm infants <29 weeks gestational age (GA) who required MV-O_2 (n=79) starting the first day of life. BPD was defined according to Jobe and Bancalari (20). Patient characteristics are outlined in **table 1 and 2**. The study was approved by the ethics committee of the Ludwig-Maximilians University in Munich (#195-07) and is in accordance with the declaration of Helsinki. Written parental informed consent was obtained in all cases. TNF-α protein expression was determined using a commercially available ELISA according to the manufacturer`s instructions (TNF-α Quantikine ELISA kit, R&D) and standardized to sIgA (Immundiagnostik AG, Bensheim, Germany) to correct for dilution effects from the suctioning procedure.

Data Analysis.

Data are given as mean ± SD. Two-way analysis of variance and the Bonferroni post-hoc test were performed to compare two groups of controls and two groups of mechanically ventilated WT (TNF-$\alpha^{+/+}$) and knockout (TNF-$\alpha^{-/-}$) newborn mice. To compare datasets from two groups of mice(immunoblot analysis), Student's unpaired t-test, or the non-parametric Mann-Whitney test (for datasets with a skewed distribution) were performed. This analysis was used as well to analyze data from patient material. Statistical analysis was done using Prism 5 software

187 package (GraphPad, San Diego, CA) and Sigma Plot v12.3 (Systat Software, San Jose, CA).

188 Differences were considered statistically significant when the p value was <0.05.

189

RESULTS

MV-O_2 induces similar impairments in the alveolar development in WT and TNF-α null mice.

Using quantitative morphometry, we found that exposing mice to MV-O_2 for 8 h impaired lung structure in both groups, resulting in a similar increase in distal airspace size and decrease in radial alveolar counts (a measure of alveolar number) in both WT (TNF-$\alpha^{+/+}$) and TNF-$\alpha^{-/-}$ mice (**Fig 1A-C**).

MV-O_2 induces a greater degree of apoptosis and inflammation in the lungs of TNF-α null versus WT mice.

Semi-quantitative analysis of TUNEL-positive cells in the lungs of ventilated newborn mice following MV-O_2 for 8h showed a 3-fold increase in apoptosis in TNF-$\alpha^{-/-}$ mice subjected to MV-O_2 when compared to ventilated WT pups **(Fig 2A, B)**. These differences were further supported by the analysis of caspase protein expression showing a significant 2- to 3-fold increase in cleaved Caspase-3, cleaved Caspase-6 and cleaved Caspase-8 in the lungs of ventilated TNF-$\alpha^{-/-}$ mice as compared to ventilated WT mice **(Fig 2C, D, E)**. Dual staining for Caspase-3 and PDGF-Rα showed a significant increase in apoptotic MFBs in the lungs of ventilated TNF-$\alpha^{-/-}$ pups as compared to unventilated control animals **(Fig 2F, G)**.

With respect to pulmonary inflammation, the number of monocytes/macrophages and neutrophils were increased in the lungs of newborn TNF-$\alpha^{-/-}$ pups after 8h of MV-O_2 (**Fig 3A, B, C**) accompanied by an increase in IL-1β, CXCL-1 and MCP-1 mRNA expression when compared to ventilated WT newborn mice (**Fig 3C**).

MV-O_2 increases activation of TGF-β signaling, and decreases NFκB activation and SMAD7 expression in lungs of TNF-$\alpha^{-/-}$ compared to WT mice.

Analysis of TGF-β signaling in the lungs of ventilated newborn mice showed a significant 3-fold increase in pSMAD 2/3 expression in newborn TNF-$\alpha^{-/-}$ mice as compared to WT pups (**Fig 4A, B**) in line with a significant increase in TGF- β mRNA expression in these lungs after 8h MV-O_2 (**Fig 4C**). These findings were associated with a significant decrease in IκB phosphorylation, indicating a reduction in NF-κB activation in the lungs of newborn TNF-$\alpha^{-/-}$ pups after 8h of MV-O_2 when compared to ventilated WT mice (**Fig 4D**). Analysis of the TGF-β inhibitor SMAD-7 showed a significant reduction of its protein expression in the lungs of ventilated TNF-$\alpha^{-/-}$ when compared to WT pups (**Fig 4E**).

TNF-α treatment successfully decreases TGF-β activation and stretch-induced Caspase-3 expression in primary lung MFBs from WT and TNF- $\alpha^{-/-}$ ***mice.***

The crosstalk between the TGF-β and the TNF-α pathway was confirmed by reduced pSMAD2 protein expression in MFBs derived from WT as well as TNF-$\alpha^{-/-}$ mice upon treatment with TNF-α (100ng/ml) (**Fig 5 A, B**). Stretching primary lung MFBs *in vitro* at room air significantly increased cleaved Caspase-3 protein expression in cells derived from newborn TNF-$\alpha^{-/-}$ pups (**Fig 5E**) but not in MFBs derived from newborn WT pups (**Fig 5C**). This increase in Caspase-3 expression was prevented by the supplementation of TNF-α (100 ng/ml) prior to mechanical stretch (**Fig 5F**) or stretch along with TGF-β (**Fig 5G**) in MFBs derived from newborn TNF-$\alpha^{-/-}$ mice, whereas TNF-α treatment (100 ng/ml) in WT cells had no significant effect on the expression level of cleaved Caspase-3 (**Fig 5C**).

TNF-α levels in tracheal aspirate in preterm infants with and without BPD.

To substantiate the experimental findings in a cohort of preterm infants, we analyzed TNF-α level in tracheal aspirates at the onset and during prolonged MV-O_2. In line with our findings,

TNF-α levels were significantly reduced in tracheal aspirate samples obtained at birth from preterm infants who later developed moderate or severe BPD, compared to preterms with no or mild disease (**Fig 6**).

DISCUSSION

Clinical and experimental evidence has identified an association between increased levels of TNF-α in the lung undergoing MV-O_2 and the development of BPD, suggesting that heightened TNF-α expression may be a harbinger of BPD development (2, 17, 30, 35). Although loss of TNF-α signaling had not been previously reported to affect normal lung development at any stage, the present study demonstrates that the absence of TNF-α in the developing lung undergoing MV-O_2 results in an increase in apoptosis and inflammation associated with increased TGF-β signaling.

TNF-α, the best studied cytokine of the TNF-family, is well known for its characteristic pro-inflammatory activity in the context of different diseases (4, 9). The successful amelioration of both infectious as well as non-infectious inflammatory diseases by the inhibition of TNF-α in adult and pediatric patient cohort provided the rationale for the current study (25).

TNF-α signaling induces and perpetuates the inflammatory response, and also invokes cell death by promoting binding of the TNF receptor 1 (TNFR1) to the associated death domain proteins (1, 5, 12, 29). On the other hand, TNF-α mediated down-stream activation of the NF-κB pathway may result in pro-survival functions that have been reported by other investigators (5, 31, 32).

Here, we demonstrate in a unique *in vivo* model that the absence of TNF-α is associated with excess activation of TGF-β signaling, increased inflammatory mediator expression, accentuated apoptosis, and reduced NF-κB activity in the ventilated newborn lung.

As indicated by co-staining experiments, the process of apoptosis induced by MV-O_2 affects the PDGF-Rα positive pulmonary MFB, driving the process of alveolar septation. We

265 therefore undertook *in vitro* experiments at room air in order to study the cell specific
266 response to stretch with or without the additional application of TGF-β. In line with our *in vivo*
267 findings, the *in vitro* analysis showed an increase in caspase expression upon mechanical
268 stretch in primary lung MFBs derived from neonatal TNF-$\alpha^{-/-}$ in contrast to pulmonary MFBs
269 from WT mice. Verifying the cross-talk between the TNF-α and the TGF-β pathway in primary
270 cells derived from the newborn mouse lung, TNF-α treatment successfully reversed both,
271 increased TGF-β activation as well as excess caspase expression induced by *in vitro* stretch

272 Previous studies in mice and in humans have shown that MV-O_2 increases TGF-β
273 signaling in the lung (15, 16, 26). In these studies, heightened activation of TGF-β augments
274 pulmonary inflammation by enhancing monocyte recruitment to the lung, and increasing
275 apoptosis. As recent studies have demonstrated important anti-inflammatory, cell survival, and
276 developmental functions of NF-κB in the newborn lung (18, 23, 24), the decrease in NF-κB
277 activity we observed may further enhance the pro-apoptotic effects of heightened TGF-β
278 signaling. Furthermore, the decrease in NF-κB activity in our model was accompanied by a
279 reduction of SMAD-7 protein levels. Cross-talk between the NF-κB and the TGF-β pathways
280 has been previously demonstrated (14), with suppression of NFκB resulting in an excess in
281 TGF-β activation, thus augmenting the recruitment of inflammatory cells, and promoting pro-
282 inflammatory cytokine production and cell death induction (15, 16). Therefore, in our model,
283 reduced NF-κB activity could not only impede the development of the newborn lung and affect
284 cell survival (18) but may also promote excessive TGF-β activation, which in turn further
285 enhances the recruitment of inflammatory cells to the lung (34).

286 In concert with the effects on apoptosis and inflammation, the absence of TNF-α did
287 not result in an improvement in lung structure in neonatal mice undergoing MV-O_2. Whether

the increase in cell death in MFBs as well as in other cell types relevant for lung development is related to impaired long-term pulmonary outcome needs to be addressed in future studies.

TNF-α level obtained from tracheal aspirates in preterm infants support the hypothesis derived from the experimental studies and allow the translation of the findings into the human system. Here, lower TNF-α levels at birth in infants that later develop BPD may explain activation of the TGF-β pathway, reported by a variety of studies (15, 16, 26). Besides the immediate detrimental effects of TGF-β with the induction of apoptosis and acute inflammation, the perpetuation of the inflammatory response enhanced by TGF-β may account for the adverse long-term effects of MV-O_2 following conventional or new ventilation protocols (8, 11).

Taken together, the data presented unravel the complexity of TNF-α function in the developing lung undergoing MV-O_2 and contribute to a broader understanding of the heterogeneous impact of constitutive and induced TNF-α levels in normal and abnormal lung development. Moreover, these results suggest that upper and lower threshold levels need to be defined in keeping with the Goldilocks principle. With respect to previous studies, the unfavorable effects of TNF-α withdrawal in the developing lung may relate to the adverse reactions observed in adult patients treated with TNF-α inhibitors (10).

Future studies should address the potential for preterm infants undergoing MV-O_2 to benefit from determination of TNF-α level at birth in order to determine their risk for BPD development and consecutive treatment modifications. Considering the complexity of pulmonary TNF-α signaling and NF-κB activity at birth, TNF-α blockade as a targeted treatment option to reduce ventilator-induced lung damage and BPD needs to be carefully re-evaluated. Special consideration should be drawn to the right timing and dosing to prevent an imbalance of physiologic NF-κB and TGF-β signaling in the context of TNF-α abundance.

312 **ACKNOWLEDGMENT**

We gratefully acknowledge sample collection by the whole staff from the neonatal intensive care unit at the perinatal center in Munich Grosshadern. This study was supported by the Friedrich-Baur-Stiftung (40/2010) (HE) and the Young Investigator Grant NWG VH-NG-829 by the Helmholtz Gemeinschaft and the Helmholtz Zentrum Muenchen (AH), Germany as well as support from the NIH R01 HL122918-01 (CMA), and the Tashia and John Morgridge Faculty Scholar Fund, Stanford Child Health Research Institute (CMA).

313

REFERENCES

1. **Baader E, Toloczko A, Fuchs U, Schmid I, Beltinger C, Ehrhardt H, Debatin KM, and Jeremias I**. Tumor necrosis factor-related apoptosis-inducing ligand-mediated proliferation of tumor cells with receptor-proximal apoptosis defects. *Cancer research* 65: 7888-7895, 2005.
2. **Bhandari V**. Hyperoxia-derived lung damage in preterm infants. *Seminars in fetal & neonatal medicine* 15: 223-229, 2010.
3. **Bland RD, Ertsey R, Mokres LM, Xu L, Jacobson BE, Jiang S, Alvira CM, Rabinovitch M, Shinwell ES, and Dixit A**. Mechanical ventilation uncouples synthesis and assembly of elastin and increases apoptosis in lungs of newborn mice. Prelude to defective alveolar septation during lung development? *American journal of physiology Lung cellular and molecular physiology* 294: L3-14, 2008.
4. **Bradley JR**. TNF-mediated inflammatory disease. *The Journal of pathology* 214: 149-160, 2008.
5. **Brenner D, Blaser H, and Mak TW**. Regulation of tumour necrosis factor signalling: live or let die. *Nature reviews Immunology* 15: 362-374, 2015.
6. **Brew N, Hooper SB, Allison BJ, Wallace MJ, and Harding R**. Injury and repair in the very immature lung following brief mechanical ventilation. *American journal of physiology Lung cellular and molecular physiology* 301: L917-926, 2011.
7. **Carraro S, Filippone M, Da Dalt L, Ferraro V, Maretti M, Bressan S, El Mazloum D, and Baraldi E**. Bronchopulmonary dysplasia: the earliest and perhaps the longest lasting obstructive lung disease in humans. *Early human development* 89 Suppl 3: S3-5, 2013.
8. **Claure N, and Bancalari E**. New modes of mechanical ventilation in the preterm newborn: evidence of benefit. *Arch Dis Child Fetal Neonatal Ed* 92: F508-512, 2007.
9. **Damas P, Reuter A, Gysen P, Demonty J, Lamy M, and Franchimont P**. Tumor necrosis factor and interleukin-1 serum levels during severe sepsis in humans. *Critical care medicine* 17: 975-978, 1989.
10. **Day R**. Adverse reactions to TNF-alpha inhibitors in rheumatoid arthritis. *Lancet* 359: 540-541, 2002.
11. **Eber E, and Zach MS**. Long term sequelae of bronchopulmonary dysplasia (chronic lung disease of infancy). *Thorax* 56: 317-323, 2001.
12. **Ehrhardt H, Fulda S, Schmid I, Hiscott J, Debatin KM, and Jeremias I**. TRAIL induced survival and proliferation in cancer cells resistant towards TRAIL-induced apoptosis mediated by NF-kappaB. *Oncogene* 22: 3842-3852, 2003.
13. **Emery JL, and Mithal A**. The number of alveoli in the terminal respiratory unit of man during late intrauterine life and childhood. *Archives of disease in childhood* 35: 544-547, 1960.
14. **Freudlsperger C, Bian Y, Contag Wise S, Burnett J, Coupar J, Yang X, Chen Z, and Van Waes C**. TGF-beta and NF-kappaB signal pathway cross-talk is mediated through TAK1 and SMAD7 in a subset of head and neck cancers. *Oncogene* 32: 1549-1559, 2013.
15. **Hilgendorff A, Parai K, Ertsey R, Jain N, Navarro EF, Peterson JL, Tamosiuniene R, Nicolls MR, Starcher BC, Rabinovitch M, and Bland RD**. Inhibiting lung elastase activity enables lung growth in mechanically ventilated newborn mice. *American journal of respiratory and critical care medicine* 184: 537-546, 2011.
16. **Hilgendorff A, Parai K, Ertsey R, Juliana Rey-Parra G, Thebaud B, Tamosiuniene R, Jain N, Navarro EF, Starcher BC, Nicolls MR, Rabinovitch M, and Bland RD**. Neonatal mice genetically modified to express the elastase inhibitor elafin are protected against the

adverse effects of mechanical ventilation on lung growth. *American journal of physiology Lung cellular and molecular physiology* 303: L215-227, 2012.
17. **Hillman NH, Moss TJ, Kallapur SG, Bachurski C, Pillow JJ, Polglase GR, Nitsos I, Kramer BW, and Jobe AH**. Brief, large tidal volume ventilation initiates lung injury and a systemic response in fetal sheep. *Am J Respir Crit Care Med* 176: 575-581, 2007.
18. **Iosef C, Alastalo TP, Hou Y, Chen C, Adams ES, Lyu SC, Cornfield DN, and Alvira CM**. Inhibiting NF-kappaB in the developing lung disrupts angiogenesis and alveolarization. *American journal of physiology Lung cellular and molecular physiology* 302: L1023-1036, 2012.
19. **Jobe AH**. The new bronchopulmonary dysplasia. *Current opinion in pediatrics* 23: 167-172, 2011.
20. **Jobe AH, and Bancalari E**. Bronchopulmonary dysplasia. *American journal of respiratory and critical care medicine* 163: 1723-1729, 2001.
21. **Liu YY, Liao SK, Huang CC, Tsai YH, Quinn DA, and Li LF**. Role for nuclear factor-kappaB in augmented lung injury because of interaction between hyperoxia and high stretch ventilation. *Translational research : the journal of laboratory and clinical medicine* 154: 228-240, 2009.
22. **Lv S, Han M, Yi R, Kwon S, Dai C, and Wang R**. Anti-TNF-alpha therapy for patients with sepsis: a systematic meta-analysis. *International journal of clinical practice* 68: 520-528, 2014.
23. **McKenna S, Michaelis KA, Agboke F, Liu T, Han K, Yang G, Dennery PA, and Wright CJ**. Sustained hyperoxia-induced NF-kappaB activation improves survival and preserves lung development in neonatal mice. *American journal of physiology Lung cellular and molecular physiology* 306: L1078-1089, 2014.
24. **Michaelis KA, Agboke F, Liu T, Han K, Muthu M, Galambos C, Yang G, Dennery PA, and Wright CJ**. IkappaBbeta-mediated NF-kappaB activation confers protection against hyperoxic lung injury. *American journal of respiratory cell and molecular biology* 50: 429-438, 2014.
25. **Monaco C, Nanchahal J, Taylor P, and Feldmann M**. Anti-TNF therapy: past, present and future. *International immunology* 27: 55-62, 2015.
26. **Morty RE, Konigshoff M, and Eickelberg O**. Transforming growth factor-beta signaling across ages: from distorted lung development to chronic obstructive pulmonary disease. *Proceedings of the American Thoracic Society* 6: 607-613, 2009.
27. **Rizzo AN, Sammani S, Esquinca AE, Jacobson JR, Garcia JG, Letsiou E, and Dudek SM**. Imatinib attenuates inflammation and vascular leak in a clinically relevant two-hit model of acute lung injury. *American journal of physiology Lung cellular and molecular physiology* 309: L1294-1304, 2015.
28. **Scherle W**. A simple method for volumetry of organs in quantitative stereology. *Mikroskopie* 26: 57-60, 1970.
29. **Sedger LM, and McDermott MF**. TNF and TNF-receptors: From mediators of cell death and inflammation to therapeutic giants - past, present and future. *Cytokine & growth factor reviews* 25: 453-472, 2014.
30. **Speer CP**. Pulmonary inflammation and bronchopulmonary dysplasia. *Journal of perinatology : official journal of the California Perinatal Association* 26 Suppl 1: S57-62; discussion S63-54, 2006.
31. **Suominen JS, Wang Y, Kaipia A, and Toppari J**. Tumor necrosis factor-alpha (TNF-alpha) promotes cell survival during spermatogenesis, and this effect can be blocked by

infliximab, a TNF-alpha antagonist. *European journal of endocrinology / European Federation of Endocrine Societies* 151: 629-640, 2004.
32. **Venkatachalam K, Venkatesan B, Valente AJ, Melby PC, Nandish S, Reusch JE, Clark RA, and Chandrasekar B**. WISP1, a pro-mitogenic, pro-survival factor, mediates tumor necrosis factor-alpha (TNF-alpha)-stimulated cardiac fibroblast proliferation but inhibits TNF-alpha-induced cardiomyocyte death. *The Journal of biological chemistry* 284: 14414-14427, 2009.
33. **Woods SJ, Waite AA, O'Dea KP, Halford P, Takata M, and Wilson MR**. Kinetic profiling of in vivo lung cellular inflammatory responses to mechanical ventilation. *American journal of physiology Lung cellular and molecular physiology* 308: L912-921, 2015.
34. **Wright CJ, and Kirpalani H**. Targeting inflammation to prevent bronchopulmonary dysplasia: can new insights be translated into therapies? *Pediatrics* 128: 111-126, 2011.
35. **Yoon BH, Romero R, Jun JK, Park KH, Park JD, Ghezzi F, and Kim BI**. Amniotic fluid cytokines (interleukin-6, tumor necrosis factor-alpha, interleukin-1 beta, and interleukin-8) and the risk for the development of bronchopulmonary dysplasia. *American journal of obstetrics and gynecology* 177: 825-830, 1997.

FIGURE LEGENDS

Figure 1 MV-O_2 impairs alveolar structure in TNF-$\alpha^{-/-}$ and WT mice.

MV-O_2 for 8h increased airspace size and decreased alveolar number in both newborn TNF-$\alpha^{-/-}$ as well as WT mice. (**A**) Representative lung tissue sections (200X) from 6-7d-old WT and TNF-$\alpha^{-/-}$ mice after MV-O_2 for 8h, showing increased air space size in both groups when compared with unventilated controls that breathed 40% O_2 for 8h. (**B**) Summary data (mean & SD) for alveolar area, assessed by quantitative image analysis of lung tissue sections showed an increase of alveolar area after MV-O_2 of TNF-$\alpha^{-/-}$ mice for 8h when compared to respective controls, whereas there was no significant change in lungs of WT littermates when compared to TNF-$\alpha^{-/-}$ mice upon MV-O_2 for 8h. Significant difference between groups, * $p < 0.05$; n = 4-8/group. (**C**) Summary data (mean & SD) for radial alveolar counts, an index of alveolar number, in lung tissue sections from WT and TNF-$\alpha^{-/-}$ mice after 8h of MV-O_2, compared with unventilated controls spontaneously breathing 40% O_2 for 8h. Significant difference between groups, *** $p < 0.001$; n = 4-8/group.

Figure 2. MV-O_2 increases apoptosis in lungs of TNF-$\alpha^{-/-}$ compared to WT mice.

(A) TUNEL staining of lung tissue sections, showing an increased number of apoptotic cells (black arrows) in the lungs of 6-7d-old TNF-$\alpha^{-/-}$ pups after 8h of MV-O_2 when compared to ventilated WT mice. **(B)** Quantitative image analysis of TUNEL positive cells indicating a significant increase in apoptosis in lungs of TNF-$\alpha^{-/-}$ mice when compared to WT littermates after 8h of MV-O_2. Significant difference between groups, ** $p < 0.01$, **** $p < 0.0001$; n = 4-7/group. Immunoblot for protein expression showed a significant increase of pulmonary Caspase-8 **(C)**, Caspase-3 **(D)** and Caspase-6 **(E)** protein expression in newborn TNF-$\alpha^{-/-}$

mice when compared to WT littermates after 8h of MV-O_2. Significant difference between groups, * $p < 0.05$; n =4/group. **(F)** Immunofluorescence image of lung tissue (400X, merged) showed increased dual staining for cleaved Caspase-3 (red) and PDGF-Rα (green) in the lungs of 6-7d-old TNF-$\alpha^{-/-}$ mice after 8h MV-O_2 (right panel) when compared to unventilated controls (left panel); white arrows indicate single (left) and dual (right) positive cells; nuclear counterstain with DAPI (blue). **(G)** Quantification of the images indicated an increase in dual positive cells per high power field in 6-7d-old TNF-$\alpha^{-/-}$ mice after 8h MV-O_2. Significant difference between groups, * $p < 0.05$; n =4/group; 10 high power fields analyzed per mouse.

Figure 3. MV-O_2 increases number of infiltrating monocytes and heightens cytokine expression in lungs of TNF-$\alpha^{-/-}$ compared to WT mice.

(A) F4/80 immunhistochemistry in PFA-fixed lung sections, showing increased pulmonary infiltration of macrophages (black arrows) in TNF-$\alpha^{-/-}$ newborn mice after MV-O_2 for 8 hours when compared to WT mice. Quantitative image analysis of **(B)** F4/80-positive cells and **(C)** number of neutrophils per 100 alveoli demonstrated a significant increase in numbers of monocytes/macrophages and neutrophils in the lungs of TNF-$\alpha^{-/-}$ when compared to WT mice. Significant difference between groups, * $p < 0.05$, **** $p < 0.0001$; n = 3-5/group. **(D)** In line with this, pulmonary mRNA expression of interleukin-1beta (IL-1β), chemokine (C-X-C motif) ligand-1 (CXCL-1) and monocyte chemotactic protein 1 (MCP-1) were increased in newborn TNF-$\alpha^{-/-}$ mice upon MV-O_2 for 8 hours in contrast to WT pups. Significant difference between groups, ** $p<0.01$, *** $p<0.001$. **** $p<0.0001$; n = 4/group.

Figure 4. MV-O_2 increases activation of TGF-β signaling, and decreases NFκB activation and SMAD7 expression in lungs of TNF-$\alpha^{-/-}$ compared to WT mice.

(A) Quantitative image analysis of pSMAD2 staining per total tissue indicated a significant increase of pSMAD2 expression in the lung periphery of TNF-$\alpha^{-/-}$ mice when compared to WT littermates after 8h of MV-O_2. Significant difference between groups, **** $p < 0.0001$; n = 5-6/group. **(B)** These results were confirmed by immunoblot analysis showing a significant increase of pSMAD2 protein expression in the lungs newborn TNF-$\alpha^{-/-}$ mice undergoing in contrast to WT pups. **(C)** MV-O_2 for 8 hours resulted in increased transforming growth factor (TGF)-β mRNA expression. Significant difference between groups, * $p<0.05$, **** $p<0.0001$; n = 4/group. **(D)** Downstream, MV-O_2 for 8 hours reduced the expression of phosphorylated IκB, indicating a reduced activation of NF-κB in the lungs of newborn TNF-$\alpha^{-/-}$ mice when compared to WT pups. Significant difference between groups, # $p=0.0501$; n = 3/group. **(E)** These results were accompanied by a significant decrease in SMAD7 protein expression in the lungs of newborn TNF-$\alpha^{-/-}$ mice when compared to WT pups. Significant difference between groups, * $p<0.05$; n = 4/group.

Figure 5. TNF- α treatment decreases TGF-β activation and stretch-induced Caspase-3 expression in primary lung MFBs from WT and TNF- $\alpha^{-/-}$ mice.

Confirming the interaction between the TNF-α and the TGF-β pathway, immunoblot analysis showed a reduction in pSMAD2 protein expression after TNF-α treatment (100 ng/ml TNF-α in H_2O + 0.1% BSA) in primary lung MFBs isolated from WT **(A)** and TNF-$\alpha^{-/-}$ **(B)** mice when compared to untreated MFBs. Significant difference between groups, * $p<0.05$, ** $p<0.01$; n = 3 mice/group. In line with this, primary lung MFBs derived from TNF-$\alpha^{-/-}$ mice revealed a significant increase of Caspase-3 protein expression upon mechanical stretch **(E)**, reversed

by TNF-α treatment (at the onset of stretch) **(F)** in contrast to the effect in MFBs isolated from WT mice, where Caspase-3 expression remained unchanged **(C, D)**. Significant difference between groups, * $p<0.05$; n = 3-4/group. Likewise, TNF-α treatment in primary lung MFBs from TNF-$\alpha^{-/-}$ mice prior to TGF-β application along with *in vitro* stretch successfully reduced Caspase-3 expression when compared to untreated cells **(G)**. Significant difference between groups, * $p<0.05$; n = 4 mice/group.

Figure 6. TNF-α levels in tracheal aspirates associated with the development of BPD.

Significantly reduced TNF-α levels at birth in tracheal aspirates obtained from preterm infants later developing moderate or severe BPD as compared to infants with no or mild disease (20). Significant difference between groups, *** $p<0.001$; n=79 preterm infants.

Figure 7.

Schematic model of the anticipated pathophysiologic process derived from the results of the experimental studies.

Table 1. Patient characteristics no/mild BPD.

Depicted are the clinical characteristics of the cohort fulfilling the diagnostic criteria of no or mild BPD (20). m=male, f=female, incomplete=incomplete course of two dosages of corticosteroids within 48 hours, complete=complete course of antenatal steroids, ventilatory support=any form of mechanical ventilator support including CPAP and oxygen therapy. All preterm infants received surfactant therapy.

Table 2. Patient characteristics moderate/severe BPD.

Depicted are the clinical characteristics of the cohort fulfilling the diagnostic criteria of moderate or severe BPD (20). m=male, f=female, incomplete=incomplete course of two dosages of corticosteroids within 48 hours, complete=complete course of antenatal steroids, ventilatory support=any form of mechanical ventilator support including CPAP and oxygen therapy. All preterm infants received surfactant therapy.

Fig 1

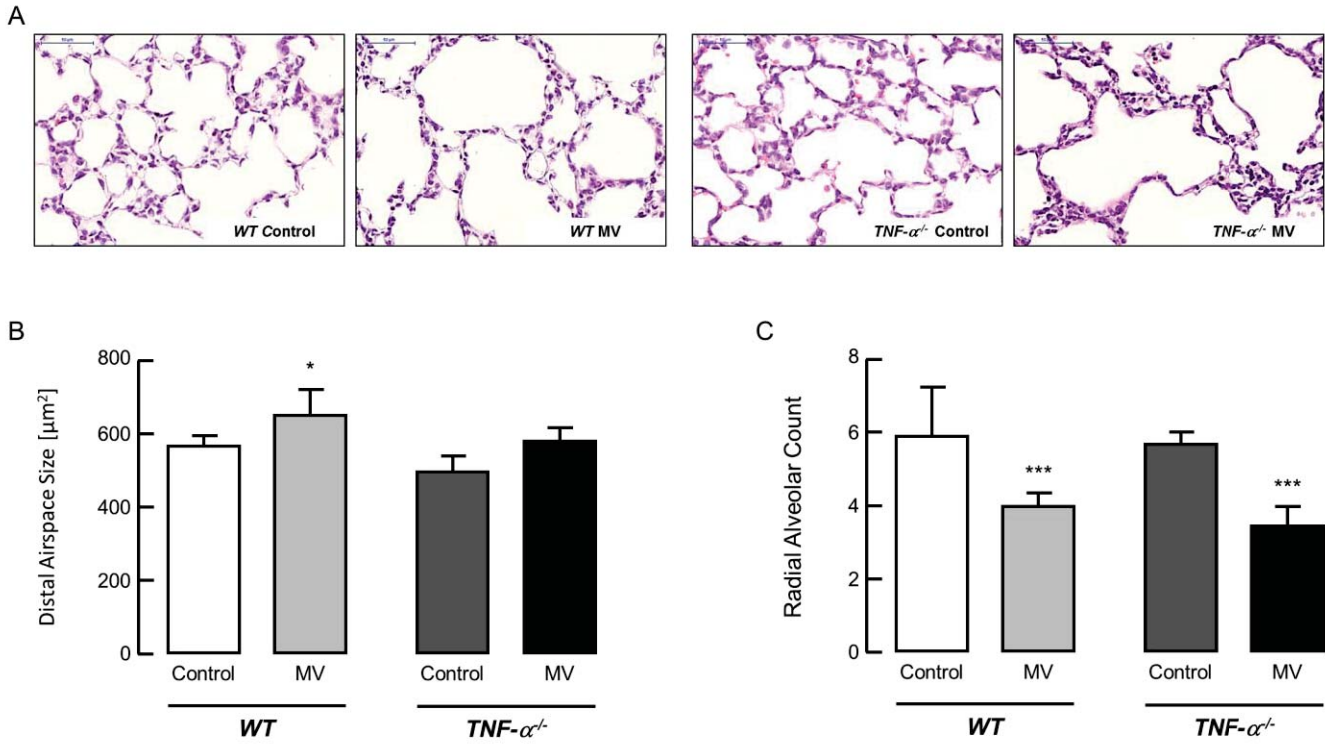
A
WT Control
WT MV
TNF-α-/- Control
TNF-α-/- MV
B
Distal Airspace Size [μm2]
800
600
400
200
0
*
Control
MV
Control
MV
WT
TNF-α-/-
C
Radial Alveolar Count
8
6
4
2
0
***
***
Control
MV
Control
MV
WT
TNF-α-/-

Fig 2

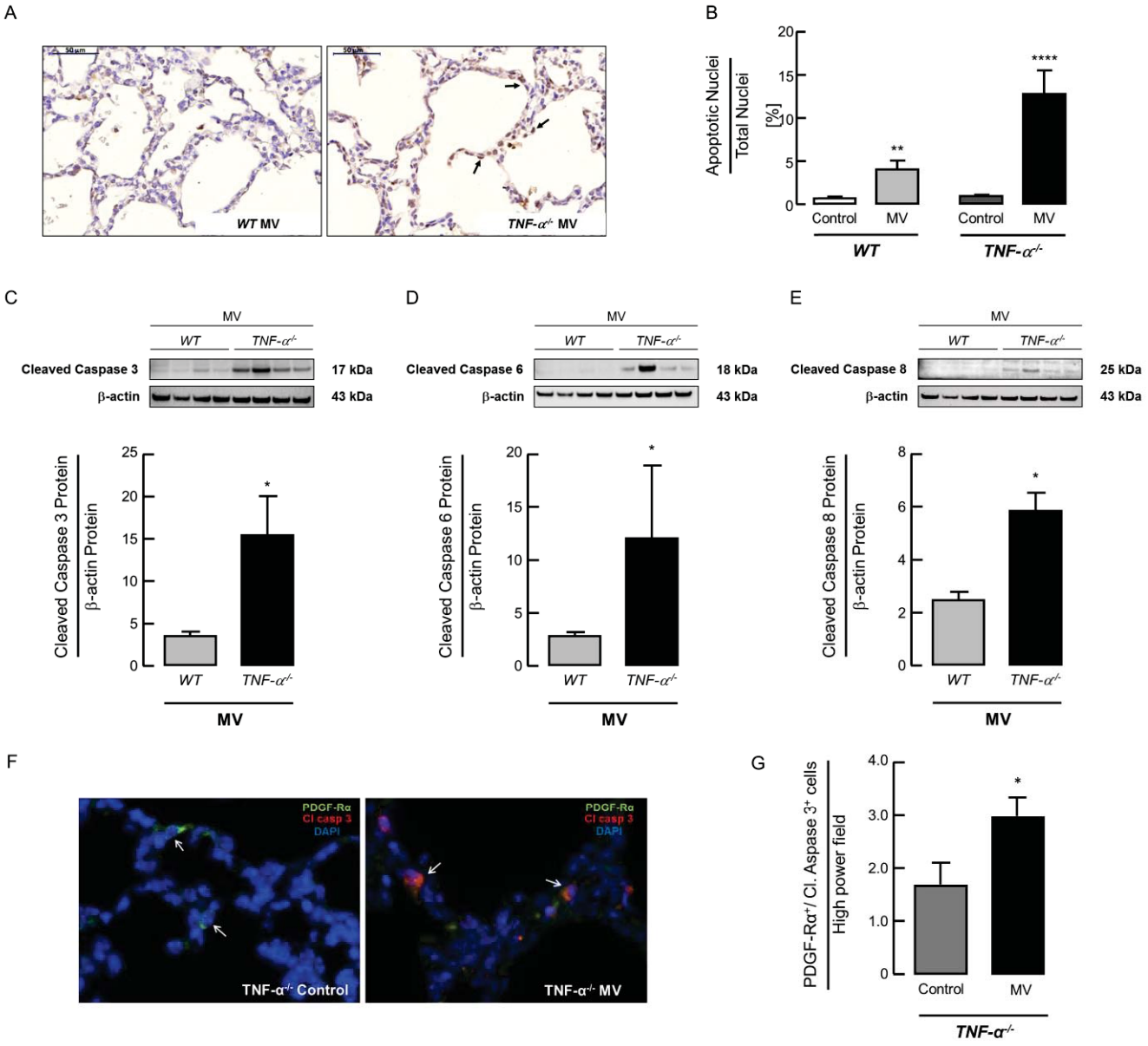
A
WT MV
TNF-α-/- MV
B
Apoptotic Nuclei / Total Nuclei [%]
Control
MV
WT
TNF-α-/-
C
MV
WT
TNF-α-/-
Cleaved Caspase 3
17 kDa
β-actin
43 kDa
Cleaved Caspase 3 Protein / β-actin Protein
D
Cleaved Caspase 6
18 kDa
Cleaved Caspase 6 Protein / β-actin Protein
E
Cleaved Caspase 8
25 kDa
Cleaved Caspase 8 Protein / β-actin Protein
F
PDGF-Rα
Cl casp 3
DAPI
TNF-α-/- Control
TNF-α-/- MV
G
PDGF-Rα+/ Cl. Aspase 3+ cells / High power field

Fig 3

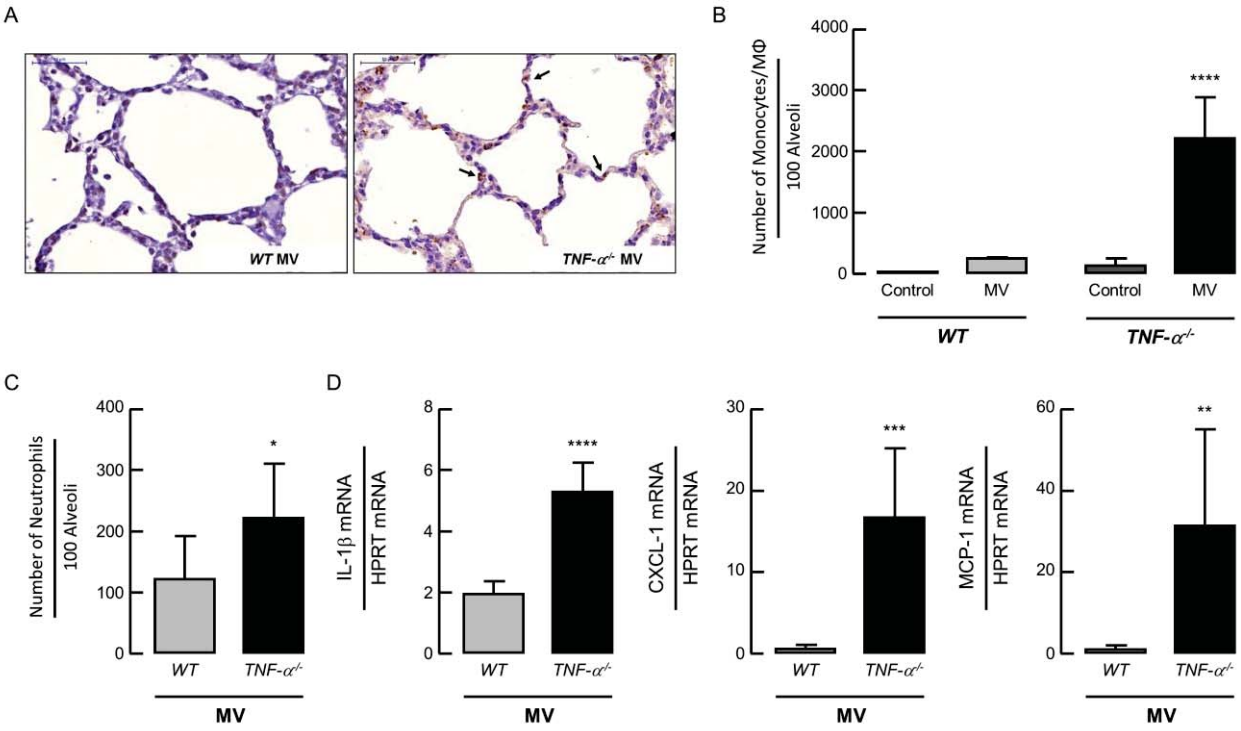
A
WT MV
TNF-α-/- MV
B
Number of Monocytes/MΦ
100 Alveoli
4000
3000
2000
1000
0
****
Control
MV
Control
MV
WT
TNF-α-/-
C
Number of Neutrophils
100 Alveoli
400
300
200
100
0
*
WT
TNF-α-/-
MV
D
IL-1β mRNA
HPRT mRNA
8
6
4
2
0
****
WT
TNF-α-/-
MV
CXCL-1 mRNA
HPRT mRNA
30
20
10
0
***
WT
TNF-α-/-
MV
MCP-1 mRNA
HPRT mRNA
60
40
20
0
**
WT
TNF-α-/-
MV

Fig 4

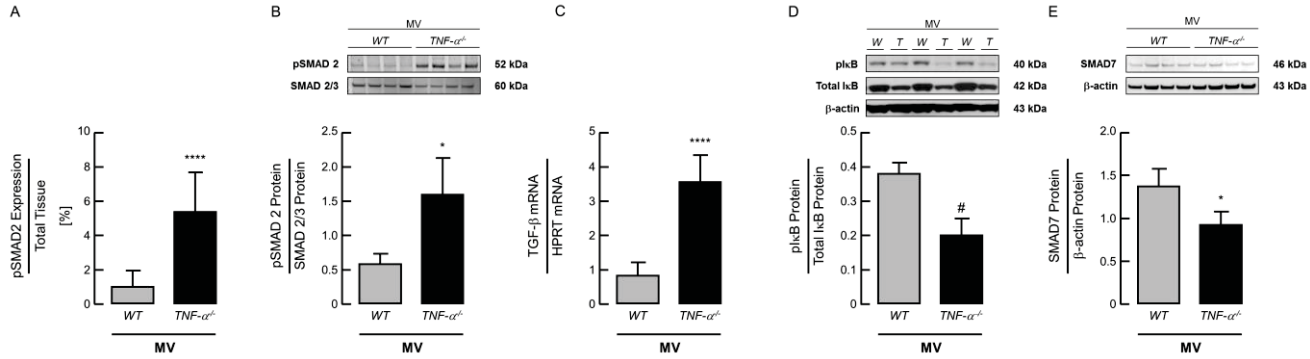
A
pSMAD2 Expression / Total Tissue [%]
****
WT
TNF-α-/-
MV
B
MV
WT
TNF-α-/-
pSMAD 2
SMAD 2/3
52 kDa
60 kDa
pSMAD 2 Protein / SMAD 2/3 Protein
*
C
TGF-β mRNA / HPRT mRNA
****
D
MV
W T W T W T
pIκB
Total IκB
β-actin
40 kDa
42 kDa
43 kDa
pIκB Protein / Total IκB Protein
#
E
MV
WT
TNF-α-/-
SMAD7
β-actin
46 kDa
43 kDa
SMAD7 Protein / β-actin Protein
*

Fig 5

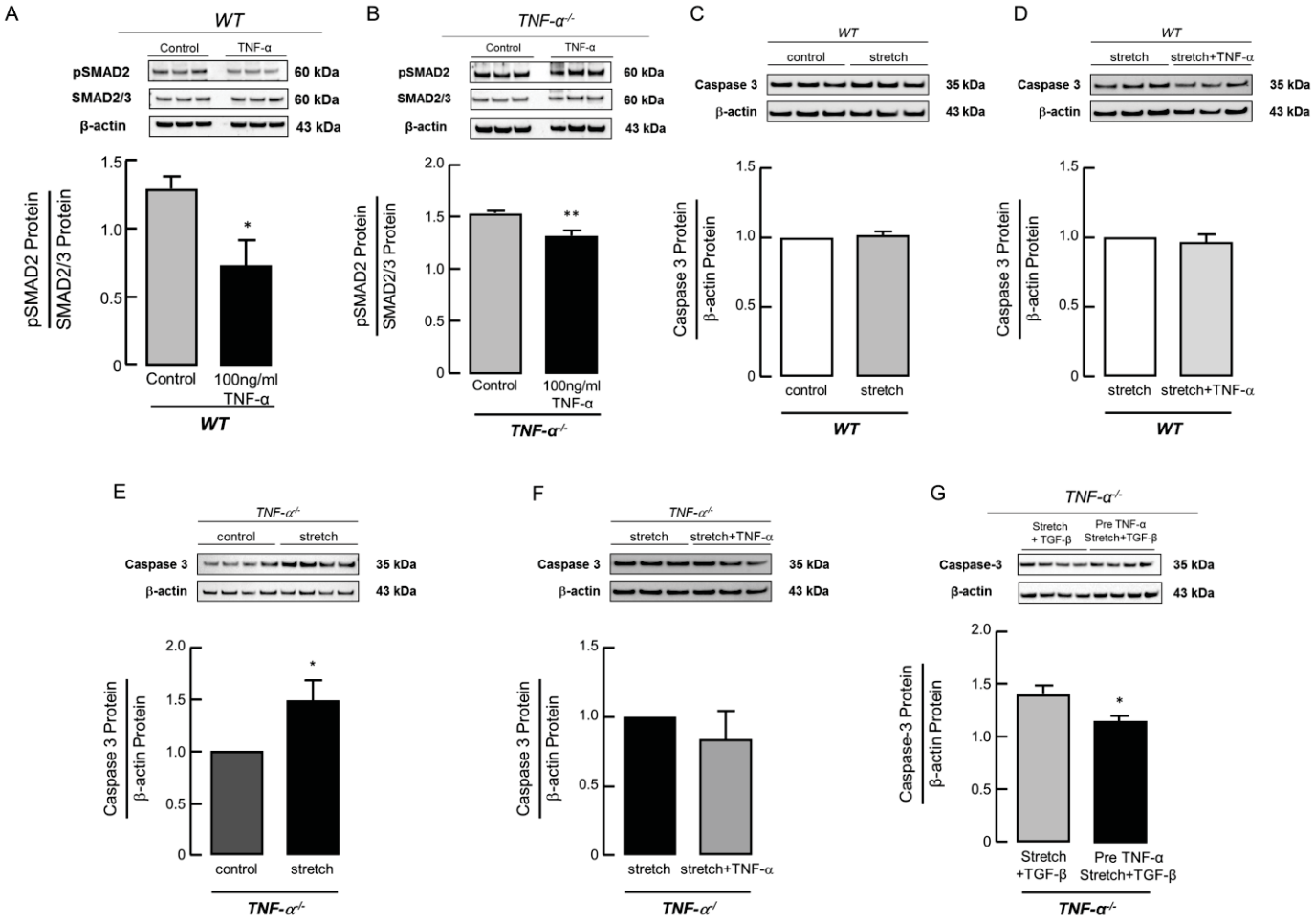
A
WT
Control
TNF-α
pSMAD2
SMAD2/3
β-actin
60 kDa
60 kDa
43 kDa
pSMAD2 Protein / SMAD2/3 Protein
Control
100ng/ml TNF-α
WT
B
TNF-α-/-
Control
TNF-α
pSMAD2
SMAD2/3
β-actin
60 kDa
60 kDa
43 kDa
pSMAD2 Protein / SMAD2/3 Protein
Control
100ng/ml TNF-α
TNF-α-/-
C
WT
control
stretch
Caspase 3
β-actin
35 kDa
43 kDa
Caspase 3 Protein / β-actin Protein
control
stretch
WT
D
WT
stretch
stretch+TNF-α
Caspase 3
β-actin
35 kDa
43 kDa
Caspase 3 Protein / β-actin Protein
stretch
stretch+TNF-α
WT
E
TNF-α-/-
control
stretch
Caspase 3
β-actin
35 kDa
43 kDa
Caspase 3 Protein / β-actin Protein
control
stretch
TNF-α-/-
F
TNF-α-/-
stretch
stretch+TNF-α
Caspase 3
β-actin
35 kDa
43 kDa
Caspase 3 Protein / β-actin Protein
stretch
stretch+TNF-α
TNF-α-/-
G
TNF-α-/-
Stretch + TGF-β
Pre TNF-α Stretch+TGF-β
Caspase-3
β-actin
35 kDa
43 kDa
Caspase-3 Protein / β-actin Protein
Stretch +TGF-β
Pre TNF-α Stretch+TGF-β
TNF-α-/-

Fig 6

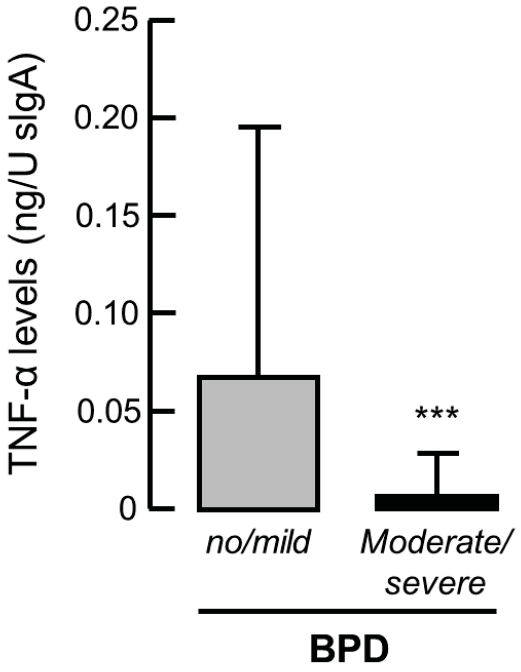
TNF-α levels (ng/U sIgA)
0.25
0.20
0.15
0.10
0.05
0
***
no/mild
Moderate/
severe
BPD

Fig 7

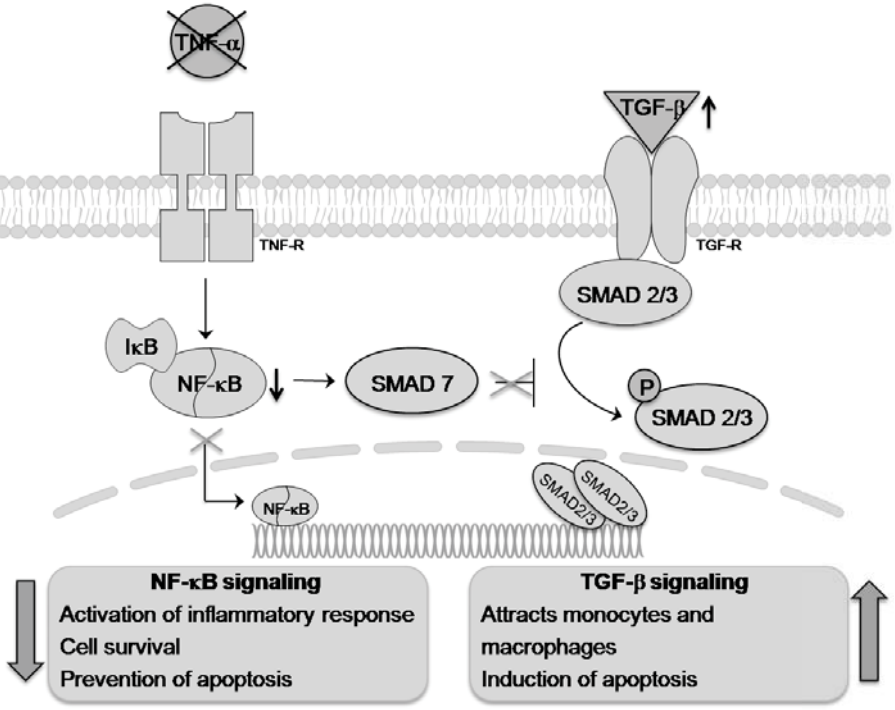
TNF-α
TGF-β
TNF-R
TGF-R
SMAD 2/3
IκB
NF-κB
SMAD 7
P
SMAD 2/3
NF-κB
SMAD2/3
SMAD2/3
NF-κB signaling
Activation of inflammatory response
Cell survival
Prevention of apoptosis
TGF-β signaling
Attracts monocytes and
macrophages
Induction of apoptosis

Table 1

patient number	gestational age (weeks)	birth weight (gms)	gender	antenatal steroids	postnatal steroids	intubated (days)	ventilatory support (days)
1	25+5	872	f	incomplete	yes	1	71
5	27+4	670	m	complete	no	6	34
6	24+2	730	m	incomplete	yes	41	69
10	28+3	1230	m	complete	no	6	37
16	27+4	950	m	incomplete	no	2	24
19	29+2	1240	f	complete	yes	4	20
24	27+1	950	m	incomplete	no	10	22
26	26+6	740	m	incomplete	yes	25	56
27	24+4	550	m	complete	yes	14	61
31	24+3	740	f	incomplete	no	19	51
33	28+3	1550	m	incomplete	no	14	19
34	28+3	1150	m	incomplete	no	1	29
37	25+3	570	m	incomplete	yes	35	66
39	26+5	985	m	complete	no	2	26
42	23+5	620	m	incomplete	yes	31	67
43	23+5	560	m	incomplete	yes	39	78
45	28+0	1050	m	incomplete	no	1	38
47	24+3	700	f	complete	no	30	44
51	25+1	680	m	incomplete	no	16	53
57	27+2	805	f	complete	yes	19	36
59	28+5	1780	m	complete	no	8	32
60	25+6	940	f	complete	yes	5	65

62	26+6	940	m	incomplete	yes	4	17
64	28+5	1340	f	incomplete	no	1	13
67	24+4	640	f	incomplete	yes	34	53
72	25+5	840	m	incomplete	no	7	58
75	26+1	880	f	complete	no	39	10
76	28+2	1150	m	complete	yes	3	20
77	28+2	1180	m	complete	no	1	9
80	28+2	1130	f	incomplete	no	2	28
89	24+1	650	f	complete	yes	24	38
92	27+4	1150	m	incomplete	no	1	26
96	27+3	1135	f	complete	no	1	17
100	28+1	1205	f	incomplete	no	6	19
105	25+5	815	f	incomplete	no	1	31
107	27+4	1110	f	incomplete	no	1	1
109	26+4	960	m	incomplete	no	3	42
110	26+4	765	m	incomplete	no	6	59
115	25+5	850	m	complete	no	2	57

Table 2

patient number	gestational age (weeks)	birth weight (gms)	gender	antenatal steroids	postnatal steroids	intubated (days)	ventilatory support (days)
7	28+0	860	f	incomplete	no	21	62
12	23+5	610	f	incomplete	yes	32	89
13	26+6	840	f	complete	no	5	65
15	27+4	810	m	incomplete	no	5	70
17	25+6	630	f	incomplete	no	1	81
18	25+6	560	f	incomplete	no	39	71
25	27+1	1060	m	incomplete	no	9	70
28	26+3	905	m	complete	yes	50	102
30	24+6	510	f	incomplete	yes	68	79
32	26+6	850	m	complete	yes	2	75
38	26+5	735	m	complete	no	10	85
48	24+5	690	m	complete	yes	34	79
49	24+3	600	f	incomplete	no	24	82
50	24+2	600	m	complete	yes	28	85
54	26+3	770	m	complete	yes	30	87
56	25+1	690	m	incomplete	yes	45	78
58	24+2	600	f	incomplete	yes	99	159
61	27+0	1050	m	complete	yes	22	66
63	28+4	540	m	incomplete	no	19	111
68	27+3	850	m	incomplete	yes	29	76
69	27+3	850	m	incomplete	yes	27	76
70	27+3	680	m	complete	no	8	64
71	27+3	790	f	complete	no	7	60

73	24+1	550	m	incomplete	yes	42	98
74	24+2	650	m	incomplete	yes	39	83
78	24+6	810	m	complete	yes	28	107
81	23+6	650	m	incomplete	yes	39	89
86	25+4	540	f	incomplete	yes	19	76
87	25+4	600	f	incomplete	yes	31	74
90	27+2	990	f	incomplete	no	79	79
93	24+2	485	m	complete	yes	37	87
94	26+1	700	m	complete	yes	22	75
95	26+1	890	m	complete	yes	25	70
99	28+1	1215	m	incomplete	no	16	58
101	24+1	570	m	incomplete	no	40	91
103	23+1	510	f	incomplete	yes	44	98
104	22+5	530	f	incomplete	yes	48	122
108	26+5	315	m	complete	no	27	133
111	27+4	960	f	incomplete	no	12	77
112	23+4	700	m	complete	yes	34	98